



Original article

Electrochemical detection of methyl-paraoxon based on bifunctional cerium oxide nanozyme with catalytic activity and signal amplification effect

Yuzhou Sun ^{a,1}, Jinchao Wei ^{a,b,1}, Jian Zou ^{b,c,1}, Zehua Cheng ^a, Zhongming Huang ^d,
Liqiang Gu ^a, Zhangfeng Zhong ^a, Shengliang Li ^d, Yitao Wang ^a, Peng Li ^{a,*}

^a State Key Laboratory of Quality Research in Chinese Medicine, Institute of Chinese Medical Sciences, University of Macau, Macau, 999078, China

^b Institute of Traditional Chinese Medicine & Natural Products, College of Pharmacy, Jinan University; Guangdong Province Key Laboratory of Pharmacodynamic Constituents of TCM and New Drugs Research, Guangzhou, 510632, China

^c Integrated Chinese and Western Medicine Postdoctoral Research Station, Jinan University, Guangzhou, 510632, China

^d Center of Super-Diamond and Advanced Films (COSDAF) and Department of Chemistry, City University of Hong Kong, Hong Kong, 999077, China

ARTICLE INFO

Article history:

Received 6 May 2020

Received in revised form

3 September 2020

Accepted 3 September 2020

Available online 8 September 2020

Keywords:

Chinese medicine

Nanozyme

Organophosphorus

Pesticide

Methyl-paraoxon

Electroanalysis

ABSTRACT

A new electrochemical sensor for organophosphate pesticide (methyl-paraoxon) detection based on bifunctional cerium oxide (CeO₂) nanozyme is here reported for the first time. Methyl-paraoxon was degraded into *p*-nitrophenol by using CeO₂ with phosphatase mimicking activity. The CeO₂ nanozyme-modified electrode was then synthesized to detect *p*-nitrophenol. Cyclic voltammetry was applied to investigate the electrochemical behavior of the modified electrode, which indicates that the signal enhancement effect may attribute to the coating of CeO₂ nanozyme. The current research also studied and discussed the main parameters affecting the analytical signal, including accumulation potential, accumulation time, and pH. Under the optimum conditions, the present method provided a wider linear range from 0.1 to 100 μmol/L for methyl-paraoxon with a detection limit of 0.06 μmol/L. To validate the proof of concept, the electrochemical sensor was then successfully applied for the determination of methyl-paraoxon in three herb samples, i.e., *Coix lacryma-jobi*, *Adenophora stricta* and *Semen nelumbinis*. Our findings may provide new insights into the application of bifunctional nanozyme in electrochemical detection of organophosphorus pesticide.

© 2020 Xi'an Jiaotong University. Production and hosting by Elsevier B.V. This is an open access article under the CC BY-NC-ND license (<http://creativecommons.org/licenses/by-nc-nd/4.0/>).

1. Introduction

Organophosphorus pesticides (OPs), as one of the most widely used pesticides in the world, have had an irreplaceable position in recent decades and the foreseeable future [1–3]. However, the widespread use of OPs has caused various degrees of contamination in Chinese medicine, food chain and the whole eco-system [4–9]. Due to their history of prevalent use, severe health effects, including neurotoxicity, embryotoxicity, genotoxicity, cytotoxicity and immunotoxicity as well as long-term effects, have been reported previously [10–13]. Among the commonly used OPs, oxo-form OPs and their active metabolites have shown the acute

toxicity on the central nervous system as well as oncogenic and teratogenic risks via phosphorylation of serine residue in the catalytic site of acetylcholinesterase [14,15]. Methyl-paraoxon (MP) is the most typical oxo-form OP which has attracted more research attention recently, not only because of its serious neurotoxicity and respiratory toxicity, but also for its common application as a nerve agent simulant to investigate structure properties of chemical warfare agents [16–18]. Consequently, to develop new and sensitive methods for MP is pivotal for health protection and public safety.

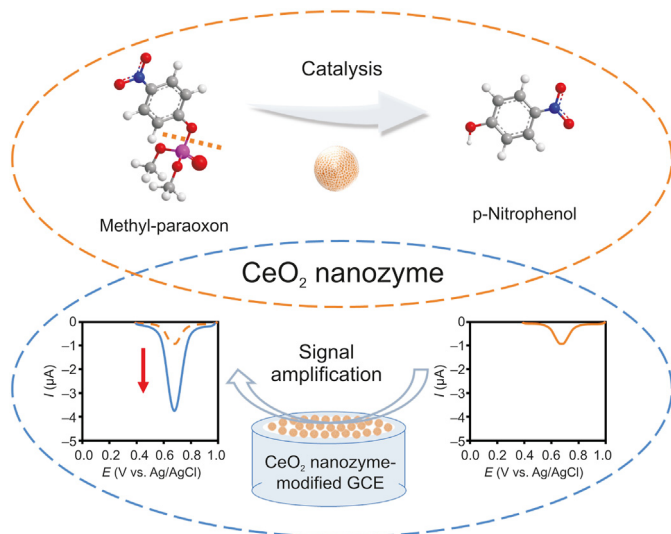
Nowadays, many analytical instrument-based methods have been established for MP detection, such as gas chromatography, liquid chromatography, and these apparatuses coupled with mass spectrometry [19,20]. These instrument-based methods can produce high accuracy results, but suffer from the drawbacks of long analysis time, requirement for skilled manpower, and the required instruments are large and expensive. Therefore, they cannot be

Peer review under responsibility of Xi'an Jiaotong University.

* Corresponding author.

E-mail address: pli1978@hotmail.com (P. Li).

¹ The three authors contributed equally to this work.



Scheme 1. Schematic illustration of the electrochemical method for methyl-paraoxon detection by using bifunctional CeO_2 nanozyme.

widely used for on-site testing. To solve this problem, rapid detection methods were designed and constructed for on-site analysis of MP as emerging technologies. Various on-site analysis methods based on the inhibition of bioenzymes activity, like acetylcholinesterase, have been applied for the rapid detection of MP [21,22]. Due to high specificity, sensitivity, simplicity, and efficiency, the enzyme-based sensing technique has become the mainstream of rapid detection. In recent years, inorganic nanomaterials have been developed for MP detection to improve the potential instability of biological enzyme and applicability of rapid detection methods [23]. Extensive nanomaterials including carbon dots, transition metal and polymer were introduced to establish various rapid detection methods for MP detection [24–27]. Nanozyme is also one kind of nanomaterials with mimic activity of biological enzyme. Due to their excellent stability, high catalytic and simple preparation, nanozymes have been widely used for the establishment of rapid detection methods [28–32]. Among these nanozymes based methods, electrochemical detection has received growing attention in recent years due to its advantages of short analysis time, high sensitivity, low cost, small sample required and easy operation [33].

To date, most of the electrochemical methods for pesticide detection have been developed based on the inhibitory mechanism of natural biological enzyme [34–37] which can be affected by many types of pollution, such as heavy metals and biological toxins. It makes the direct determination of MP lack selectivity, and even leads to false positive results. Some other researchers focused on the development and application of novel nanomaterials in electrochemical assays with signal amplification effect [38–41]. The materials formed by specific chemical reactions, like in situ generated nanozyme-initiated cascade reaction [41], can effectively complete signal amplification and obtain excellent detection results. Inspired by the utilization of nanozyme with bifunctional properties which can eliminate the shortcomings of biological enzymes and amplify the detection signal in electrochemical detection, we developed a new electrochemical technique based on the cerium oxide (CeO_2) as nanozyme for pesticide detection in this study (Scheme 1). On the one hand, CeO_2 exhibits the organophosphorus hydrolase mimicking activity, which can catalyze the decomposition of MP to generate *para*-nitrophenol (p-NP). On the other hand, the electrochemical signal of p-NP was amplified after

the nanozyme coating on the surface of electrode. As far as what is known, there has been no report on the application of bifunctional nanozyme in the pesticide detection so far.

2. Experimental

2.1. Chemicals and reagents

Hydrogen peroxide (H_2O_2 ; 30%), ammonia solution (NH_4OH ; 30%), cerium chloride ($\text{CeCl}_3 \cdot 6\text{H}_2\text{O}$; 99.95%), sodium hydroxide (NaOH ; 96%), Nafion 117 solution (5%), hydrochloric acid solution (HCl , 6 mol/L) and ethanol (99.7%) were all purchased from Shanghai Aladdin Biochemical Technology Co., Ltd. (Shanghai, China). Phosphate buffer solution (PBS) was prepared from phosphate buffered salt powder supplied by Nanjing SenBeiJia Biotechnology Co., Ltd. (Nanjing, China). Methyl-paraoxon (HPLC; 99.8%) and Tris base ($\geq 99.8\%$) were obtained from Sigma Aldrich (St. Louis, MO, USA).

2.2. Instruments

Electrochemical analysis was performed using Princeton PAR-STAT electrochemical workstation (AMETEK, Oak Ridge, TN, USA). A conventional three-electrode system was used in all electrochemical measurements, and all electrodes were obtained from Shanghai Chenhua Instrument Co., Ltd (Shanghai, China). The system consists of a 3 mm diameter glassy carbon electrode (GCE, CHI 104), a saturated calomel electrode (CHI 111) as a reference electrode, and a platinum wire counter electrode (CHI115). The transmission electron microscopy (TEM) images were obtained from transmission electron microscopy (Talos F200 \times , FEI, Waltham, MA, USA) operated at 200 kV. The crystalline features of CeO_2 nanozyme were characterized by X-ray diffraction (XRD) patterns on Bruker D8 Advance X-ray diffractometer (Smartlab, Rigaku Co., Tokyo, Japan) with $\text{Cu K}\alpha$ irradiation ($\lambda=0.15406$ nm, 40 kV, 40 mA). UV–vis absorption spectra were recorded on DR 6000 UV–vis spectrophotometer (HACH, Loveland, CO, USA).

2.3. Synthesis and preparation of CeO_2 nanozyme

The 7.5 mL of ammonium hydroxide and 2.5 mL of hydrogen peroxide (30%) were added to a solution of CeCl_3 (1.0 g) in 75 mL of deionized water with vigorous stirring. The resulting mixture was stirred at 100 °C for 1 h. Light yellow dispersion could be observed when the temperature reached 100 °C. After the chemical reaction was completed, the reactants were centrifuged and washed several

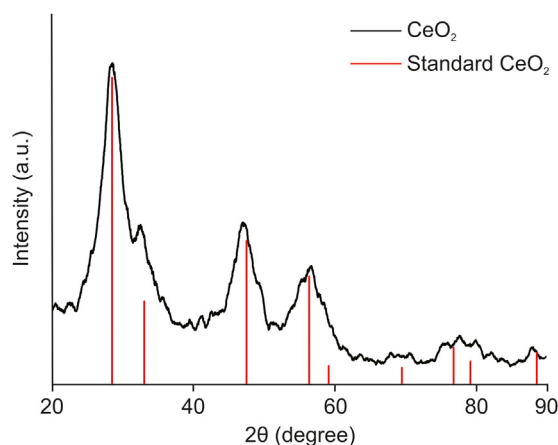


Fig. 1. X-ray diffraction (XRD) patterns of CeO_2 sample.

times with deionized water until the pH of supernatant became neutral. Finally, the solvent is removed by freeze drying for 20 h to yield the yellow nanoparticles.

2.4. Fabrication of the GCE

CeO₂ suspensions were used to modify the electrode surface by drop-casting. The GCE was polished on the felt with nano-alumina powders and thoroughly cleaned until a specular gloss was obtained. After this, further cleaning was achieved using ethanol and distilled water in ultrasonic bath to remove any traces of impurities. To form suspension, 4 mg of CeO₂ nanozyme was added to 700 μL of ethanol and 300 μL of 0.5% Nafion solution and sonicated for 30 min. The 12 μL of the resulting suspension was added dropwise to the surface of the GCE. In this way, CeO₂ nanozyme-modified GCE was prepared for further experiments.

2.5. Electrochemical detection of MP

The sample preparation procedure was carried out prior to pesticide detection according to our previous study with some modifications [42]. First, MP stock solution was diluted with 10 mM Tris solution. The above 2 mL of solution was taken and coexisted with 20 mg of CeO₂ nanozyme in centrifuged tube. After incubation in water bath at 75 °C for 1 h, the reactants were centrifuged at 15,000 rpm for 2 min. One milliliter of the obtained supernatant was diluted with 5 mL of PBS solution, and the pH was adjusted to 6 with HCl solution (1.5 mmol/L). Finally, the mixture was diluted with PBS (pH=6) to a final volume of 15 mL, obtaining the final electrochemical detection solution. All working solutions hereinafter were referred to as this one. Nitrogen blowing was carried out to exclude the influence of dissolved oxygen in the electrochemical signal.

Cyclic voltammetry (CV), electrochemical impedance spectroscopy (EIS) and differential pulse voltammetry (DPV) were the electrochemical techniques used to explore the performance of modified electrode. CV measurement was performed by potential cycling, scanning from –1.0 V to 1.0 V (vs. Ag/AgCl) at a scan rate of 50 mV/s. EIS measurement was performed as follows: the applied DC voltage at 0.25 V (vs. Ag/AgCl) with amplitude of 5 mV, and the frequency range from 0.1 Hz to 100 kHz. DPV experiments with potential from 0.0 V to 1.0 V were conducted under the following conditions of scan rate at 50 mV/s: accumulation potential at 0.4 V with accumulation time of 20 s, and modulation potential at 0.12 V.

2.6. Real sample analysis

All herb samples were purchased from a pharmacy in Macau, China. Herbal extracts were strictly prepared in accordance with the requirements of the Pharmacopoeia of the People's Republic of

China (2015 Edition) [43]. In brief, 1.5 g of accurately weighed sample with MP at different concentrations was mixed with 10 mL of water in a 50 mL centrifuge tube under ultrasonic treatment for 20 min. Subsequently, 15 mL of acetonitrile and 4 g of anhydrous magnesium sulfate were added successively and shaken vigorously. After centrifugation at 4,000 rpm for 1 min, 10 mL of collected supernatant was evaporated to dryness under a stream of nitrogen and re-dissolved with working solution. The solution was centrifuged and diluted to the final volume of 15 mL after the addition of CeO₂ nanozyme. The MP concentration in sample solution was detected by DPV with CeO₂ nanozyme-modified GCE.

3. Results and discussion

3.1. Characterization of CeO₂ nanozyme

The XRD pattern of CeO₂ is demonstrated in Fig. 1 within the 2θ range between 20° and 90°. The characteristic diffraction peaks could be indexed to the (1 1 1), (2 0 0), (2 2 0), and (3 1 1) crystal planes (JCPDS Card No. 00-004-0593). No diffraction peaks of impurities appeared, indicating high purity of the CeO₂ synthesized in this work. The physical properties and apparent structure of CeO₂ nanozyme were further investigated through TEM. As shown in Fig. 2A, good crystallinity of CeO₂ with clear lattice fringes was obtained. The lattice fringes with an interplane spacing of 0.30 nm matched with (1 1 1) plane of CeO₂ (Fig. 2A inset). The synthesized CeO₂ was uniform in size and the estimated average diameter was between 3 and 4 nm (Fig. 2B). The small and uniform particle size provides a larger specific surface area and more active sites, leading to superior enhanced performance in electrochemical detection.

3.2. Electrochemical behavior of CeO₂ nanozyme-modified GCE

The electrochemical behavior of bare GCE and CeO₂ nanozyme-modified GCE was investigated by CV. After MP was catalyzed by CeO₂ nanozyme, apparent voltammetric peaks appeared for bare GCE and the modified GCE at scan rate of 50 mV/s scanning from –1.0 V to 1.0 V (Fig. 3A). The result is consistent with the reported voltammetric peak of p-NP [44,45], indicating the prepared CeO₂ nanozyme has successfully transformed MP into p-NP. It was further verified by UV–vis experiment, which is consistent with the previous literatures [31] (Fig. S1). This phenomenon is mainly due to the coexistence of Ce(III) and Ce(IV) on the spherical CeO₂ nanozymes synthesized in this study. It is reported that surface Ce³⁺ sites could play an important role in the dephosphorylation reaction considering the biomimetic functionality of the binuclear Ce(III)–Ce(IV) complex [46]. As Ce³⁺ is usually associated with the formation of oxygen vacancy [47], spherical CeO₂ nanozymes have the highest surface density of oxygen vacancies in their various particle shapes, thus exhibiting the best dephosphorylation activity [48]. Comparing the DPV response differences between the catalyzed MP and the original MP (Fig. 3B), an additional anodic peak appeared, indicating this method successfully converted undetectable components into detectable molecules directly. Moreover, the reaction parameters were optimized for the completed decomposition of MP (Fig. S2). Finally, 20 mg CeO₂ was selected to react with MP for 1 h at 75 °C in further experiments. According to the previous electrochemical studies for the detection of MP or other pesticides with similar structure, the electrochemical response of nitro group is commonly used for sensing [49]. The characteristic cathodic peak of nitro group could be observed ranging from –0.06 to –1.0 V due to the different working solutions, which is ascribed to the transfer of four electrons and four protons accompanied with reduction of nitro-group to hydroxylamine group. In general, there are many constituents containing

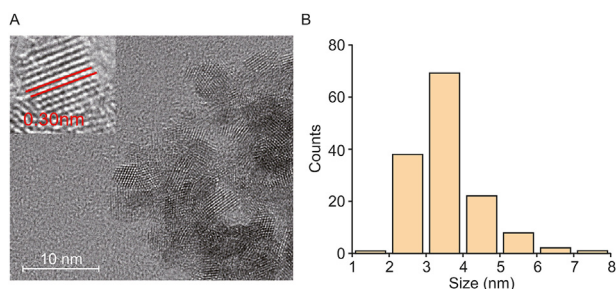


Fig. 2. (A) TEM image (inset: the lattice fringes with an interplane spacing of 0.30 nm) and (B) particle size distribution of the CeO₂.

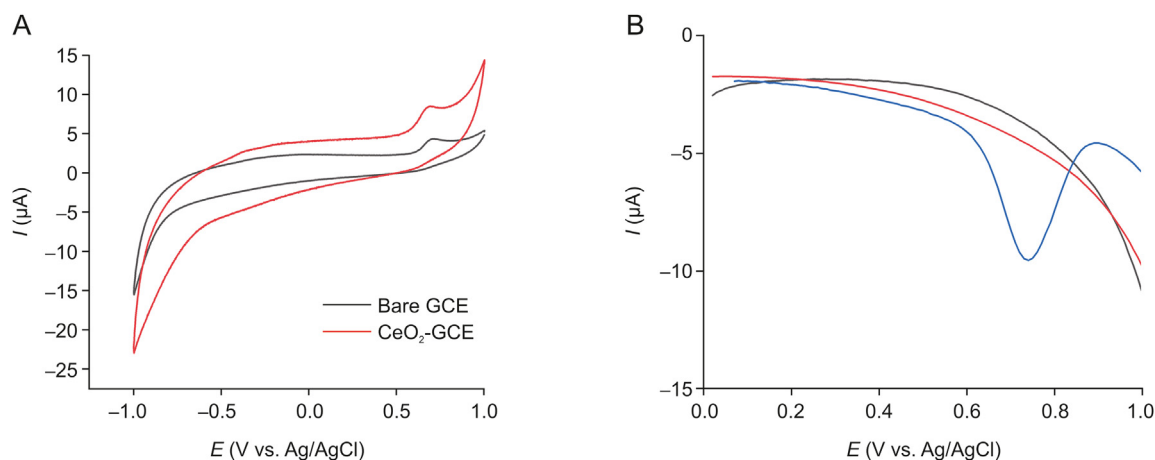
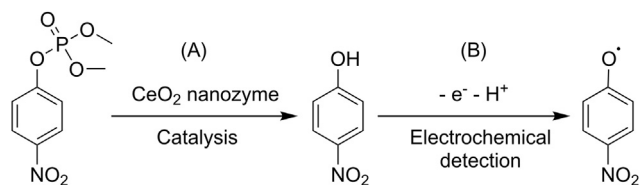


Fig. 3. (A) Cyclic voltammograms of bare GCE and CeO₂ nanozyme-modified GCE in the presence of 100 μmol/L catalyzed MP at scan rate of 50 mV/s. (B) Differential pulse voltammograms of bare GCE (gray line) and CeO₂ nanozyme-modified GCE (red line) in working buffer, and DPV of CeO₂ nanozyme-modified GCE (blue line) in the presence of 100 μmol/L catalyzed MP.



Scheme 2. (A) The catalytic process and (B) the proposed electrochemical oxidation mechanism of MP in the presence of CeO₂ nanozyme.

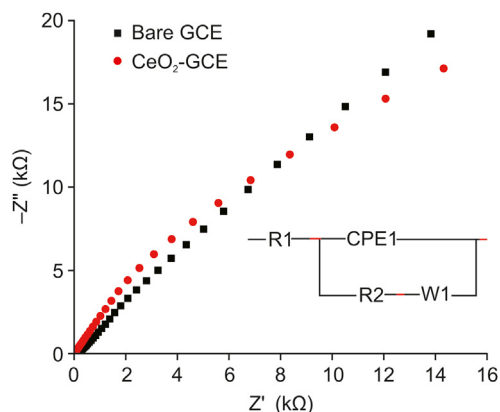


Fig. 4. Nyquist plots of bare GCE and CeO₂ nanozyme-modified GCE in the presence of 10 μmol/L catalyzed MP. (Inset) Equivalent circuit. R1: ohmic resistance; R2: charge transfer resistance; W1: Warburg impedance; CPE1: constant phase element.

nitro group existing in real samples, especially herbal plants, which would be the interferences for pesticide detection by using electrochemical method. In this study, we selected the obtained anodic peak of phenolic hydroxyl group at 0.75 V for MP detection. As shown in Scheme 2, phenolic hydroxyl group connected with phosphorus atom in the original MP molecular at first. After the reaction of CeO₂ nanozyme and MP being completed under water bath condition, the phenolic hydroxyl group could be obtained. Comparing the electrochemical signal (0.75 V) differences of sample solutions before and after treatment by CeO₂ nanozyme, MP could be detected in the real samples more clearly and sensitively.

EIS was used to characterize the detection efficiency of the

modified electrode. Fig. 4 shows the EIS result of bare GCE and CeO₂ nanozyme-modified GCE in PBS buffer (pH=6) containing 10 μmol/L catalyzed MP. As shown in inset of Fig. 4, an equivalent circuit model clearly demonstrates the EIS data, where the R1, R2, W1, and CPE represent ohmic resistance, charge transfer resistance, Warburg impedance, and constant phase element, respectively. A slight increase in R1 indicates that CeO₂ nanozymes covered on the GCE surface are good conductive materials. Meanwhile, the decrease of R2 means that the electron transfer process in CeO₂/GCE is faster than that in the GCE [50]. Our results are coincident with those of the preliminary study, which also reveal the excellent electrochemical properties of CeO₂ [51]. As is known, CeO₂ has become one of the most active oxide catalysts in the rare earth oxide series, and its characteristic properties might put down to the unique crystal structure, high oxygen storage capacity, and strong oxidation-reduction performance [52,53].

Next, the effect of scan rate ranging from 10 to 200 mV/s was investigated on the electrochemical oxidation of the catalyzed MP on the modified electrode (Fig. 5). The increase in anodic peak current corresponds with the increased scanning speed and shows a linear relationship with correlation coefficient (R^2) of 0.9954 (Fig. 5B). The similar result has been reported previously, which indicates the oxidation of p-NP is a typical adsorption controlled electrochemical process [49].

3.3. Optimization of the detection conditions

Some experimental conditions in this study were carefully explored to further enhance the electrochemical signal response, such as accumulation potential, accumulation time, and pH of the working solution.

As we mentioned above, the electrochemical oxidation of p-NP is an adsorption-controlled process. The parameters affecting adsorption process will greatly influence the sensitivity of the method. As shown in Fig. S3, the peak current increased with the enhancement of accumulation potential, indicating p-NP was absorbed on the surface of modified electrode continuously. The peak current reached the maximum value when the accumulation potential was 0.4 V. However, the peak current began to decrease as the potential continued to increase, which might be due to the adsorption of more impurities on the electrode surface [50]. Accumulation time will also affect the absorption of p-NP on the electrode surface. With the extension of accumulation time from 5 s

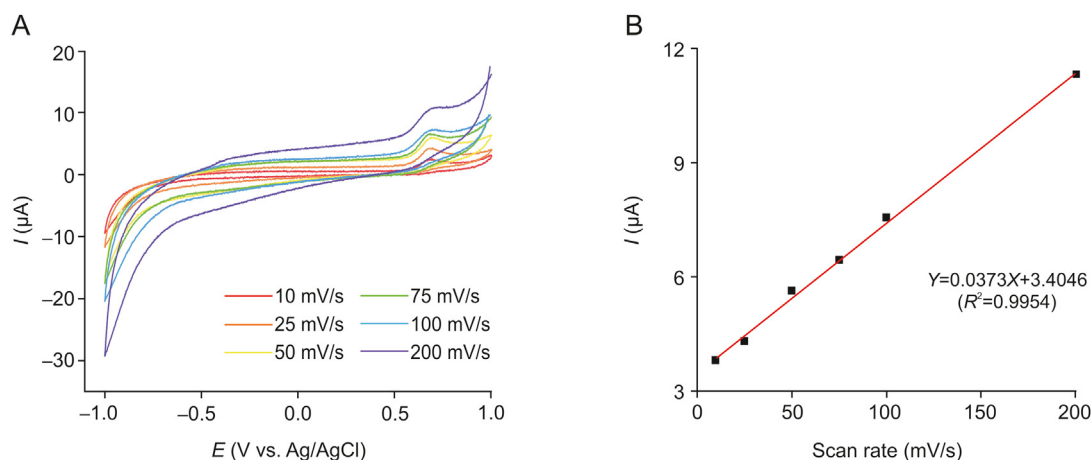


Fig. 5. (A) CV curves of CeO₂ nanozyme-modified GCE at different scan rates in range of 10–200 mV/s in working solution containing 50 μmol/L catalyzed MP. (B) Correlation between anodic peak current and scan rates.

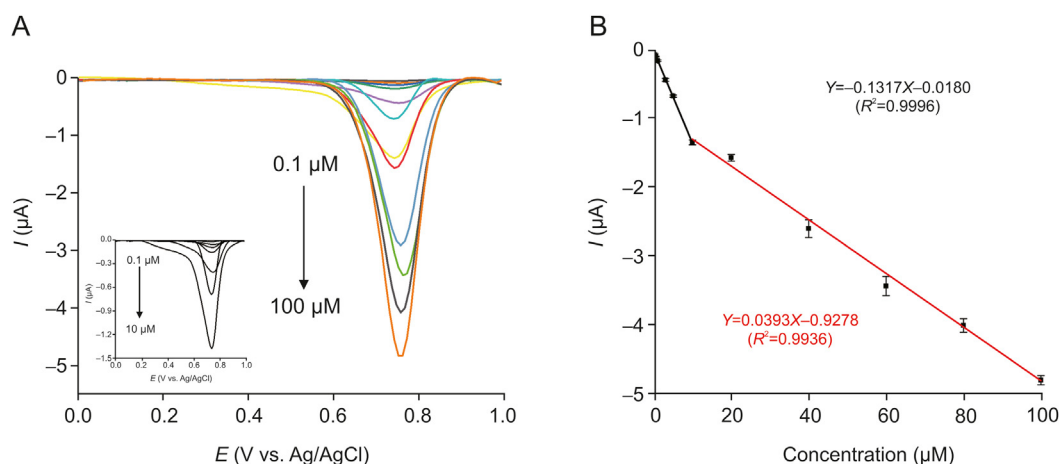


Fig. 6. (A) DPV curves of the CeO₂ nanozyme-modified GCE when the concentration of the catalyzed MP increased from 0.1 to 100 μmol/L and from 0.1 to 10 μmol/L (inset). (B) Calibration curve of peak current vs. MP concentrations.

Table 1

Comparison of different methods for pesticide detection.

Method	Detection mechanism	Analyte	Linear range	Limit of detection	Real sample	Refs.
CeO ₂ NPs-coated PAD	Visual colorimetric detection	Methyl-paraoxon	0–0.1 μg/mL	18.3 ng/mL	Cabbage, green mussel	[56]
Co ₃ O ₄ /rGO	UV–vis detection	Paraoxon	8–140 μmol/L	0.80 μmol/L	Cabbages, river, tap water	[57]
Carbon dots	Fluorescence detection	Ethyl-paraoxon	0–5.80 mmol/L	0.22 μmol/L	Bok choy	[58]
Chemical method	Colorimetric detection	Paraoxon	0.11–11.50 μmol/L	0.20 μmol/L	–	[59]
CeO ₂ nanozyme-modified GCE	Electrochemical detection	Methyl-paraoxon	0.1–100 μmol/L	0.06 μmol/L	Herbal plant (Semen nelumbinis, Coix lacryma-jobi, Adenophora stricta)	This work

PAD: paper-based analytical devices; rGo: reduced graphene oxide; GCE: glassy carbon electrode.

to 100 s, the peak current increased accordingly (Fig. S4). Considering that this method is for rapid detection, we selected 20 s as the optimal accumulation time. The acidic and alkaline condition of working solution will greatly affect the ionization of the analytes and electron transfer [54]. Thus, pH ranging from 4 to 8 was optimized in this work. The phenolic hydroxyl group of p-NP was hardly ionized under acidic condition, then the peak current was very low (Fig. S5). The peak current on the electrode surface was the highest when pH=6, indicating that p-NP could be absorbed and oxidized on the electrode surface in the near-neutral environment. This might be due to the pKa of the phenol group, and similar results have previously been obtained [55].

3.4. Electrochemical detection of MP by CeO₂ nanozyme-modified GCE

Then, the applicability of this nanozyme-assisted electrochemical method was investigated under the optimal conditions. Fig. 6 shows the DPV curves of CeO₂ nanozyme-modified GCE at different concentrations of MP. As shown in Fig. 6A, the anodic peak current increased with increased MP concentration. What's more, the oxidation peak current increased linearly with MP concentration in the ranges of 0.1–10 μmol/L and 10–100 μmol/L, with correlation coefficients (R^2) higher than 0.99 for both two analytical curves ($n=3$, Fig. 6B). The calculated detection limit was 0.06 μmol/L ($S/N=3$). This electrochemical method for the detection of MP was

Table 2
Comparison of different electrochemical detection methods for pesticide detection.

Analyte	Electrode	Linear range ($\mu\text{mol/L}$)	Limit of detection ($\mu\text{mol/L}$)	Real sample	Refs.
Methyl-paraoxon, methyl-parathion and ethyl-paraoxon	TiO ₂ @dopamine@serine/histamine/glutamic acid modified electrode	0.5–100	0.20	Vegetable (Lactuca sativa L.)	[32]
Paraoxon	Layer-by-layer assembled multi-enzyme/carbon nanotube biosensor	0.5–40	0.50	Apple	[37]
Carbaryl		10–80	10		
Carbofuran	Gold nanoparticles and graphene oxide modified screen-printed carbon electrode	1.0–250	0.22	Cucumber and rice	[40]
Chlorpyrifos	Acetylcholinesterase immobilized screen-printed electrodes	1.0–50000	0.50	Milk	[60]
Imidacloprid	Molecularly imprinted polymers and graphene modified glassy carbon electrode	0.5–15	0.10	Rice	[61]
Methyl-paraoxon	CeO ₂ nanozyme-modified glassy carbon electrode	0.1–100	0.06	Herbal plant (Semen nelumbinis, Coix lacryma-jobi, Adenophora stricta)	This work

compared with other methods in Table 1 [56–59], and also compared with the previously developed electrochemical method for MP detection in Table 2 [32,37,40,60,61]. This method exhibited the remarkable performance thanks to the good electrochemical properties of CeO₂ nanozyme and superior sensitivity of DPV method.

3.5. Anti-interference experiment

In order to further explore anti-interference capability of this method for practical application, the interference study was performed in the presence of 10 μM MP and potential interferences like Cu²⁺, Cl⁻, SO₄²⁻, Na⁺, and K⁺, respectively. DPV measurements were performed in triplicates for each sample. The selected inorganic ions demonstrated negligible disturbances on the MP detection by using this electrochemical method (Fig. 7A). Furthermore, other organophosphorus pesticides containing similar structure, such as malathion, chlorfenvinphos, ethyl-paraoxon, and fensulfothion, were selected for testing the anti-interference ability. It is found in Fig. 7B that most of those pesticides (10 μM) exhibited comparable responses with MP only at the same concentration except chlorfenvinphos. The carbon-carbon double bond connected with chlorines is the characteristic group of chlorfenvinphos, and the strong electron-withdrawing atom chlorine may promote the electron transfer from phenolic hydroxyl and then enhance the electrochemical signal in this work [62].

3.6. Real sample analysis

To verify the applicability of the developed method for MP detection, MP at different levels (0.1, 0.5, and 3.0 $\mu\text{mol/L}$) was tested in three herb samples, Coix lacryma-jobi, Adenophora stricta and Semen nelumbinis. It is evident from Table 3 that the detected values are consistent with the spiked concentrations. The recovery was presented with mean \pm standard deviation ($n=3$). The recoveries of MP in three samples ranged from 80.91% \pm 4.86% to 116.84% \pm 1.42%. According to the recoveries for pesticide analysis (70%–120%, RSD < 20%) recommended by European Commission [63], the analytical performances in all three herb samples were acceptable and also confirmed that the present work is a promising technique for MP detection in real samples even with complex matrix.

4. Conclusion

In this work, an electrochemical method involving CeO₂ nanozyme was used for MP detection. Different from other nanozymes or nanomaterials used in previous electrochemical studies, CeO₂ nanozyme in this study plays significant roles in both substrate catalysis and signal amplification. UV–vis result revealed its catalytic activity for the conversion from MP to p-NP. Voltammetric studies indicated the signal amplification function of CeO₂ nanozyme-modified GCE towards MP detection due to its improved

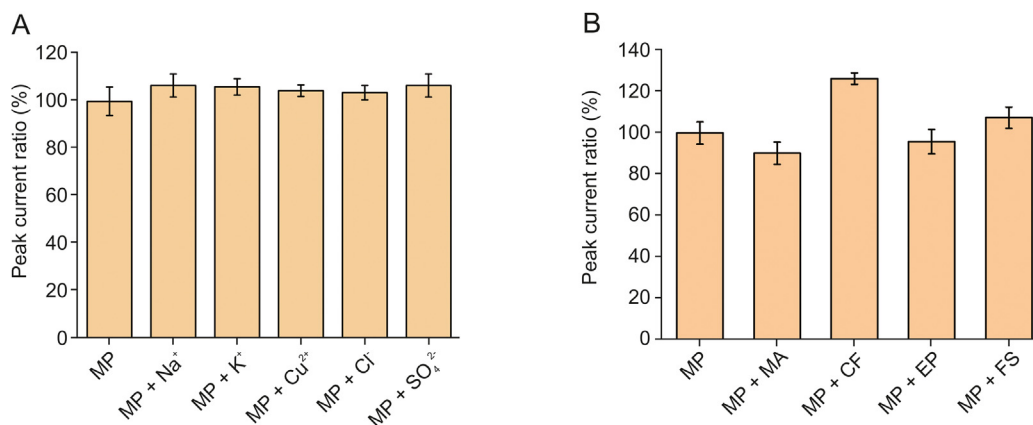


Fig. 7. The electrochemical response of MP coexists with (A) different inorganic ions or (B) other pesticide. MA: malathion; CF: chlorfenvinphos; EP: ethyl-paraoxon; FS: fensulfothion.

Table 3

The recovery detection of methyl-paraoxon using CeO₂ nanozyme-modified GCE in Chinese medicinal material samples.

Sample	Spiked (μmol/L)	Detected (μmol/L)	Recovery	
			Mean ± SD (%) ^a	RSD (%; n=3)
Semen nelumbinis	0.10	0.097	97.11 ± 3.22	3.31
	0.50	0.511	102.25 ± 6.30	6.16
	3.00	2.786	92.87 ± 3.18	3.43
Coix lacryma-jobi	0.10	0.105	105.13 ± 4.19	3.98
	0.50	0.446	89.25 ± 2.21	5.48
	3.00	3.337	111.23 ± 7.64	6.87
Adenophora stricta	0.10	0.117	116.84 ± 1.42	7.21
	0.50	0.469	93.72 ± 9.21	9.82
	3.00	2.427	80.91 ± 4.86	6.00

^a Standard deviation of three determinations.

electrochemical properties. Under the optimized conditions, the present method offers high stability, wide response range and lower LOD. The desirable recoveries in different herbal samples show the potential of CeO₂ for practical applications. In summary, all the experimental results we have collected suggest that this CeO₂ nanozyme-modified electrochemical method is an attractive candidate for MP analysis with simplicity, rapidity, and sensitivity. Nevertheless, we believe there is still room for the present method to improve. To elaborate further, CeO₂ nanozyme in this work was used at two steps independently: sample preparation and detection procedure. The small amount of CeO₂ loaded on the electrode cannot guarantee the catalytic reaction completely, while the increased CeO₂ decreased the electronic conductivity and affected the signal enhancement effect. In the future, it might be possible to develop the electrochemical method with dual functions of catalysis and detection by supporting CeO₂ on porous materials or three-dimensional materials with a large surface area.

Declaration of competing interest

The authors declare that there are no conflicts of interest.

Acknowledgments

This work was supported by Macau Science and Technology Development Fund (Grant No.: 0147/2019/A3), Guangxi Innovation-driven Development Special Foundation Project (Project No.: GuiKe AA18118049), China Postdoctoral Science Foundation (Grant No.: 2019M653299), and the National Natural Science Foundation of China (Grant No.: 81903794).

Appendix A. Supplementary data

Supplementary data to this article can be found online at <https://doi.org/10.1016/j.jpha.2020.09.002>.

References

- M.-Y. Yoon, B. Cha, J.-C. Kim, Recent trends in studies on botanical fungicides in agriculture, *Plant Pathol. J.* 29 (2013) 1–9.
- A. Derbalah, R. Chidya, W. Jadoon, et al., Temporal trends in organophosphorus pesticides use and concentrations in river water in Japan, and risk assessment, *J. Environ. Sci.* 79 (2019) 135–152.
- Y. Li, M. Wan, G. Yan, et al., A dual-signal sensor for the analysis of parathion-methyl using silver nanoparticles modified with graphitic carbon nitride, *J. Pharm. Anal.* 11 (2021) 183–190.
- V. Tripathy, B.B. Basak, T.S. Varghese, et al., Residues and contaminants in medicinal herbs-A review, *Phytochem. Lett.* 14 (2015) 67–78.
- L.F. Alfonso, G.V. Germán, P.C. María del Carmen, et al., Adsorption of organophosphorus pesticides in tropical soils: the case of karst landscape of northwestern Yucatan, *Chemosphere* 166 (2017) 292–299.
- K. Seebunrueng, Y. Santaladchaiyakit, S. Srijaranai, Vortex-assisted low density solvent liquid–liquid microextraction and salt-induced demulsification coupled to high performance liquid chromatography for the determination of five organophosphorus pesticide residues in fruits, *Talanta* 132 (2015) 769–774.
- S. Li, P. Yu, C. Zhou, et al., Analysis of pesticide residues in commercially available chenpi using a modified QuEChERS method and GC-MS/MS determination, *J. Pharm. Anal.* 10 (2020) 60–69.
- C.M. Liu, J.A. Qin, X.W. Dou, et al., Extrinsic harmful residues in Chinese herbal medicines: types, detection, and safety evaluation, *Chin. Herb. Med.* 10 (2018) 117–136.
- L. Wang, W. Kong, M. Yang, et al., Safety issues and new rapid detection methods in traditional Chinese medicinal materials, *Acta Pharm. Sin. B* 5 (2015) 38–46.
- D. Wessels, D.B. Barr, P. Mendola, Use of biomarkers to indicate exposure of children to organophosphate pesticides: implications for a longitudinal study of children's environmental health, *Environ. Health Perspect.* 111 (2003) 1939–1946.
- M.A. van den Dries, M. Guxens, A. Pronk, et al., Organophosphate pesticide metabolite concentrations in urine during pregnancy and offspring attention-deficit hyperactivity disorder and autistic traits, *Environ. Int.* 131 (2019), 105002.
- F. Holme, B. Thompson, S. Holte, et al., The role of diet in children's exposure to organophosphate pesticides, *Environ. Res.* 147 (2016) 133–140.
- M. Edleston, N.A. Buckley, P. Eyer, et al., Management of acute organophosphorus pesticide poisoning, *Lancet* 371 (2008) 597–607.
- J.A. Crow, V. Bittles, K.L. Herring, et al., Inhibition of recombinant human carboxylesterase 1 and 2 and monoacylglycerol lipase by chlorpyrifos oxon, paraoxon and methyl paraoxon, *Toxicol. Appl. Pharmacol.* 258 (2012) 145–150.
- S.A. Quandt, M.A. Hernández-Valero, J.G. Grzywacz, et al., Workplace, household, and personal predictors of pesticide exposure for farmworkers, *Environ. Health Perspect.* 114 (2006) 943–952.
- P. Houze, A. Hutin, M. Lejay, et al., Comparison of the respiratory toxicity and total cholinesterase activities in dimethyl versus diethyl paraoxon-poisoned rats, *Toxicology* 7 (2019), 23.
- D.E. Lorke, G.A. Petroianu, The experimental oxime K027—a promising protector from organophosphate pesticide poisoning. A review comparing K027, K048, pralidoxime, and obidoxime, *Front. Neurosci.* 13 (2019), 427.
- T. Myhrer, P. Aas, Pretreatment and prophylaxis against nerve agent poisoning: are undesirable behavioral side effects unavoidable? *Neurosci. Biobehav. Rev.* 71 (2016) 657–670.
- P. Parrilla Vázquez, C. Ferrer, M.J. Martínez Bueno, et al., Pesticide residues in spices and herbs: sample preparation methods and determination by chromatographic techniques, *Trac. Trends Anal. Chem.* 115 (2019) 13–22.
- A. Samsidar, S. Siddiquee, S.M. Shaarani, A review of extraction, analytical and advanced methods for determination of pesticides in environment and foodstuffs, *Trends Food Sci. Technol.* 71 (2018) 188–201.
- J. Wang, W. Lv, J. Wu, et al., Electropolymerization-Induced positively charged phenothiazine polymer photoelectrode for highly sensitive photoelectrochemical biosensing, *Anal. Chem.* 91 (2019) 13831–13837.
- J. Chang, H. Li, T. Hou, et al., Paper-based fluorescent sensor for rapid naked-eye detection of acetylcholinesterase activity and organophosphorus pesticides with high sensitivity and selectivity, *Biosens. Bioelectron.* 86 (2016) 971–977.
- G. Aragay, F. Pino, A. Merkoçi, Nanomaterials for sensing and destroying pesticides, *Chem. Rev.* 112 (2012) 5317–5338.
- X. Yan, Y. Song, C. Zhu, et al., MnO₂ nanosheet-carbon dots sensing platform for sensitive detection of organophosphorus pesticides, *Anal. Chem.* 90 (2018) 2618–2624.
- S. Cinti, G. Valdés-Ramírez, W. Gao, et al., Microengine-assisted electrochemical measurements at printable sensor strips, *Chem. Commun.* 51 (2015) 8668–8671.
- W.E. Liu, Z. Chen, L.P. Yang, et al., Molecular recognition of organophosphorus compounds in water and inhibition of their toxicity to acetylcholinesterase, *Chem. Commun.* 55 (2019) 9797–9800.
- J. Xu, C. Yu, T. Feng, et al., N-Carbamoylmaleimide-treated carbon dots: stabilizing the electrochemical intermediate and extending it for the ultrasensitive detection of organophosphate pesticides, *Nanoscale* 10 (2018) 19390–19398.
- Y. Huang, J. Ren, X. Qu, Nanozymes: classification, catalytic mechanisms, activity regulation, and applications, *Chem. Rev.* 119 (2019) 4357–4412.
- D. Jiang, D. Ni, Z.T. Rosenkrans, et al., Nanozyme: new horizons for responsive biomedical applications, *Chem. Soc. Rev.* 48 (2019) 3683–3704.
- J. Wu, X. Wang, Q. Wang, et al., Nanomaterials with enzyme-like characteristics (nanozymes): next-generation artificial enzymes (II), *Chem. Soc. Rev.* 48 (2019) 1004–1076.
- J. Wei, L. Yang, M. Luo, et al., Nanozyme-assisted technique for dual mode detection of organophosphorus pesticide, *Ecotoxicol. Environ. Saf.* 179 (2019) 17–23.
- L.H. Qiu, P. Lv, C. Zhao, et al., Electrochemical detection of organophosphorus pesticides based on amino acids conjugated nanoenzyme modified electrodes, *Sensor. Actuator. B Chem.* 286 (2019) 386–393.
- M. Govindhan, B.-R. Adhikari, A. Chen, Nanomaterials-based electrochemical detection of chemical contaminants, *RSC Adv.* 4 (2014) 63741–63760.

- [34] F. Zhao, Y. Yao, X. Li, et al., Metallic transition metal dichalcogenide nano-sheets as an effective and biocompatible transducer for electrochemical detection of pesticide, *Anal. Chem.* 90 (2018) 11658–11664.
- [35] Q. Zhang, Q. Xu, Y. Guo, et al., Acetylcholinesterase biosensor based on the mesoporous carbon/ferroferic oxide modified electrode for detecting organophosphorus pesticides, *RSC Adv.* 6 (2016) 24698–24703.
- [36] E.A. Songa, J.O. Okonkwo, Recent approaches to improving selectivity and sensitivity of enzyme-based biosensors for organophosphorus pesticides: a review, *Talanta* 155 (2016) 289–304.
- [37] Y. Zhang, M.A. Arugula, M. Wales, et al., A novel layer-by-layer assembled multi-enzyme/CNT biosensor for discriminative detection between organophosphorus and non-organophosphorus pesticides, *Biosens. Bioelectron.* 67 (2015) 287–295.
- [38] M. Khairy, A.A. Khorshed, F.A. Rashwan, et al., Sensitive determination of amlodipine besylate using bare/unmodified and DNA-modified screen-printed electrodes in tablets and biological fluids, *Sensor. Actuator. B Chem.* 239 (2017) 768–775.
- [39] L. Tian, J. Qi, K. Qian, et al., An ultrasensitive electrochemical cytosensor based on the magnetic field assisted binanozymes synergistic catalysis of Fe₃O₄ nanozyme and reduced graphene oxide/molybdenum disulfide nanozyme, *Sensor. Actuator. B Chem.* 260 (2018) 676–684.
- [40] A. Jirasirichote, E. Punrat, A. Suea-Ngam, et al., Voltammetric detection of carbofuran determination using screen-printed carbon electrodes modified with gold nanoparticles and graphene oxide, *Talanta* 175 (2017) 331–337.
- [41] X. Wang, W. Lv, J. Wu, et al., In situ generated nanozyme-initiated cascade reaction for amplified surface plasmon resonance sensing, *Chem. Commun.* 56 (2020) 4571–4574.
- [42] J. Wei, Y. Yang, J. Dong, et al., Fluorometric determination of pesticides and organophosphates using nanoceria as a phosphatase mimic and an inner filter effect on carbon nanodots, *Microchim. Acta* 186 (2019), 66.
- [43] Chinese Pharmacopoeia Commission, Pharmacopoeia of the People's Republic of China: 2015 Edition, Vol. 1, People's Medical Publishing House, Co., Ltd., Beijing, 2015, pp. 392–393.
- [44] S.-Q. Hu, J.-W. Xie, Q.-H. Xu, et al., A label-free electrochemical immunosensor based on gold nanoparticles for detection of paraoxon, *Talanta* 61 (2003) 769–777.
- [45] M. Pontić, G. Thouand, F. De Nardi, et al., Antipassivating electrochemical process of glassy carbon electrode (GCE) dedicated to the oxidation of nitrophenol compounds, *Electroanalysis* 23 (2011) 1579–1584.
- [46] M.H. Kuchma, C.B. Komanski, J. Colon, et al., Phosphate ester hydrolysis of biologically relevant molecules by cerium oxide nanoparticles, *Nanomed-Nanotechnol.* 6 (2010) 738–744.
- [47] J. Paier, C. Penschke, J. Sauer, Oxygen defects and surface chemistry of ceria: quantum chemical studies compared to experiment, *Chem. Rev.* 113 (2013) 3949–3985.
- [48] M.J. Manto, P. Xie, C. Wang, Catalytic dephosphorylation using ceria nanocrystals, *ACS Catal.* 7 (2017) 1931–1938.
- [49] V. Velusamy, S. Palanisamy, S.-W. Chen, et al., Novel electrochemical synthesis of cellulose microfiber entrapped reduced graphene oxide: a sensitive electrochemical assay for detection of fenitrothion organophosphorus pesticide, *Talanta* 192 (2019) 471–477.
- [50] M. Khairy, H.A. Ayoub, C.E. Banks, Non-enzymatic electrochemical platform for parathion pesticide sensing based on nanometer-sized nickel oxide modified screen-printed electrodes, *Food Chem.* 255 (2018) 104–111.
- [51] C. Walkey, S. Das, S. Seal, et al., Catalytic properties and biomedical applications of cerium oxide nanoparticles, *Environ. Sci.-Nano.* 2 (2015) 33–53.
- [52] D.R. Mullins, The surface chemistry of cerium oxide, *Surf. Sci. Rep.* 70 (2015) 42–85.
- [53] F. Charbgo, M. Ramezani, M. Darroudi, Bio-sensing applications of cerium oxide nanoparticles: advantages and disadvantages, *Biosens. Bioelectron.* 96 (2017) 33–43.
- [54] M. Santhiago, C.S. Henry, L.T. Kubota, Low cost, simple three dimensional electrochemical paper-based analytical device for determination of p-nitrophenol, *Electrochim. Acta* 130 (2014) 771–777.
- [55] K.C. Honeychurch, J.P. Hart, Voltammetric behavior of p-nitrophenol and its trace determination in human urine by liquid chromatography with a dual reductive mode electrochemical detection system, *Electroanalysis* 19 (2007) 2176–2184.
- [56] S. Nouanthavong, D. Nacapricha, C.S. Henry, et al., Pesticide analysis using nanoceria-coated paper-based devices as a detection platform, *Analyst* 141 (2016) 1837–1846.
- [57] T. Wang, J. Wang, Y. Yang, et al., Co₃O₄/Reduced graphene oxide nanocomposites as effective phosphotriesterase mimetics for degradation and detection of paraoxon, *Ind. Eng. Chem. Res.* 56 (2017) 9762–9769.
- [58] M.M.F. Chang, I.R. Ginjom, S.M. Ng, Single-shot 'turn-off' optical probe for rapid detection of paraoxon-ethyl pesticide on vegetable utilising fluorescence carbon dots, *Sensor. Actuator. B Chem.* 242 (2017) 1050–1056.
- [59] M.-P.N. Bui, A. Abbas, Simple and rapid colorimetric detection of p-nitrophenyl substituent organophosphorus nerve agents, *Sensor. Actuator. B Chem.* 207 (2015) 370–374.
- [60] D. Catalina Rodríguez, S. Carvajal, G. Peñuela, Effect of chlorpyrifos on the inhibition of the enzyme acetylcholinesterase by cross-linking in water-supply samples and milk from dairy cattle, *Talanta* 111 (2013) 1–7.
- [61] M. Zhang, H.T. Zhao, T.J. Xie, et al., Molecularly imprinted polymer on graphene surface for selective and sensitive electrochemical sensing imidacloprid, *Sensor. Actuator. B Chem.* 252 (2017) 991–1002.
- [62] D. Gonçalves-Filho, C.C.G. Silva, D. De Souza, Pesticides determination in foods and natural waters using solid amalgam-based electrodes: challenges and trends, *Talanta* 212 (2020), 120756.
- [63] European Commission, Guidance Document on Analytical Quality Control and Method Validation Procedures for Pesticide Residues and Analysis in Food and Feed: SANTE/11813/2017, http://www.eurl-pesticides.eu/docs/public/tmp/PLT_article.asp?CntID=727. (Accessed 1 November 2019).